ORIGINAL ARTICLE

Real-Time State Estimation and Long-Term Model Adaptation: A Two-Sided Approach toward Personalized Diagnosis of Glucose and Insulin Levels

Claudia Eberle, Dr. med.,[1] and Christoph Ament, Prof. Dr.-Ing. habil.[2]

Abstract

Background:

With continuous glucose sensors (CGSs), it is possible to obtain a dynamical signal of the patient's subcutaneous glucose concentration in real time. How could that information be exploited? We suggest a model-based diagnosis system with a twofold objective: real-time state estimation and long-term model parameter identification.

Methods:

To obtain a dynamical model, Bergman's nonlinear minimal model (considering plasma glucose G, insulin I, and interstitial insulin X) is extended by two states describing first and second insulin response. Furthermore, compartments for oral glucose and subcutaneous insulin inputs as well as for subcutaneous glucose measurement are added. The observability of states and external inputs as well as the identifiability of model parameters are assessed using the empirical observability Gramian. Signals are estimated for different nondiabetic and diabetic scenarios by unscented Kalman filter.

Results:

(1) Observability of different state subsets is evaluated, e.g., from CGSs, $\{G, I\}$ or $\{G, X\}$ can be observed and the set $\{G, I, X\}$ cannot. (2) Model parameters are included, e.g., it is possible to estimate the second-phase insulin response gain k_{G2} additionally. This can be used for model adaptation and as a diagnostic parameter that is almost zero for diabetes patients. (3) External inputs are considered, e.g., oral glucose is theoretically observable for nondiabetic patients, but estimation scenarios show that the time delay of 1 h limits application.

Conclusions:

A real-time estimation of states (such as plasma insulin I) and parameters (such as k_{G2}) is possible, which allows an improved real-time state prediction and a personalized model.

J Diabetes Sci Technol 2012;6(5):1148-1158

Author Affiliations: [1]Department of Medicine, University of California, San Diego, La Jolla, California; and [2]Institut for Automation and Systems Engineering, Ilmenau University of Technology, Ilmenau, Germany

Corresponding Author: Christoph Ament, Prof. Dr.-Ing. habil., Institut for Automation and Systems Engineering, Ilmenau University of Technology, Helmholtzplatz 5, D–98693 Ilmenau, Germany; email address *ament@web.de*

Real-Time State Estimation and Long-Term Model Adaptation: A Two-Sided
Approach toward Personalized Diagnosis of Glucose and Insulin Levels

Eberle

Introduction

Continuous glucose sensors (CGSs) are able to measure a subcutaneous glucose concentration with a comparatively high sampling frequency, typically in time intervals of 5 min. These data can either be evaluated online (i.e., in real time), in order to control glucose thresholds and to give an alert in cases of hypoglycemia or hyperglycemia, or it can be used offline, in order to analyze glucose profiles by patient or by physician *a posteriori*, in order to optimize insulin therapy. These concepts are summarized as continuous glucose monitoring (CGM).[1]

The disadvantages of a CGS are possible deviations in the measured glucose amplitude and a delay of the signal compared with plasma glucose.[2,3] Concepts such as deconvulation[4] and Kalman filtering[5–10] have been developed to determine the plasma glucose more accurately with a CGS.

We state that glucose dynamics, which are now available from CGSs for the first time in real time, may provide much more information on the patient's glucose–insulin system if it is evaluated based on an appropriate dynamical model. **Figure 1** shows the suggested setup of the model-based diagnosis system. For *state estimation* and *parameter identification*, the same signals are made available, which are the interstitial glucose measurement from the CGS, the current model information, and, if necessary, external inputs.

But both units work on different time scales. State estimation provides real-time information, which is required for alerts or for predictions. To develop closed-loop concepts,[11,12] a model-predictive controller may also utilize these model-based predictions in real time.[13] The corresponding structure is in line with that suggested by El-Khatib and colleagues,[14] but we will not focus on closed-loop control. The *parameter identification* unit estimates long-term changes of the glucose–insulin system. The estimate of model parameters will be used for model adaption, which is typically updated in a daily rate, and may support a physician in diagnosing the development of insulin resistance or diabetes.

Nevertheless, analysis tools and algorithms for both units will be developed in the following sections using consistent tools. In the next section, a common model is defined, which is used for observability analysis and
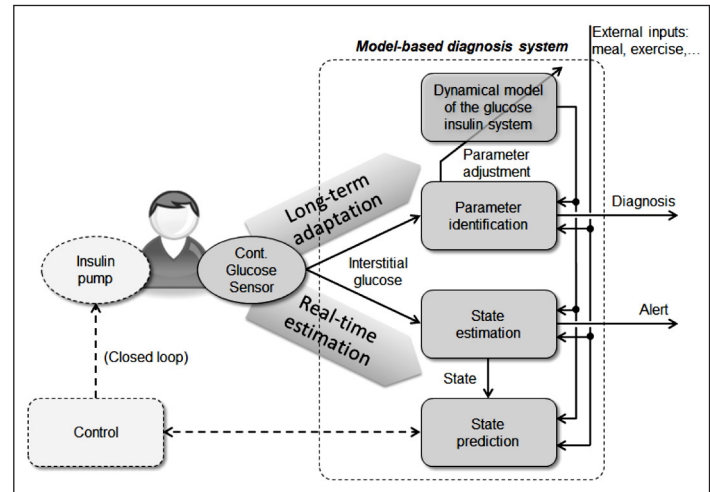

Figure 1. Setup of a model-based diagnosis system. State estimation and parameter identification are running in parallel but on different time scales. The state estimation provides a real-time estimate of the glucose–insulin status, which is required for alerts, prediction, and closed-loop approaches. Parameter identification determines long-term estimates of the model parameters. They can be used for diagnosis and model adjustment.

real-time estimation. This is then extended to parameter identification and input estimation.

Methods

A Mathematical Model of the Glucose–Insulin System

In contrast with general model approaches such as ARMAX models[15–17] or neural nets, we suggest a physiological model approach. The first three states of the model are the core states of the insulin glucose homeostasis and follow the concept introduced by Bergman.[18–20] The glucose and insulin concentrations in the plasma are denoted by $G(t)$ and $I(t)$, respectively (see block diagram in **Figure 2**). Two additional inputs, $u_{GV}(t)$ and $u_{GI}(t)$, are introduced such that an intravenous glucose tolecance test (IVGTT) and an intravenous insulin dosage can be modeled. The insulin-triggered glucose degradation is assigned to the interstitial tissue. The interstitial insulin concentration is denoted by $X(t)$, and its feedback to the glucose system is shown in the control block of **Figure 2**. Note that $X(t)$ is defined in the same units as $I(t)$, and all states are defined as differences to their basal values. This does not change system dynamics but simplifies model equations.

Real-Time State Estimation and Long-Term Model Adaptation: A Two-Sided
Approach toward Personalized Diagnosis of Glucose and Insulin Levels

Eberle

We extended Bergman's model approach using two further states in order to distinguish the first- and second-phase insulin response.[21] The transfer functions of this pancreatic regulation process are also shown in the control block of **Figure 2**. This realizes the feedback of the glucose to the insulin system. The glucose–insulin interplay is completely described at this point.

Furthermore, interfaces to model the excitation and measurement of this system must be added. The gastro-enterological system is modeled as a second-order delay system (**Figure 2**). By its input $u_{GO}(t)$, an oral glucose tolerance test (OGTT) can be modeled. For diabetes patients who apply insulin bolus, input $u_{IS}(t)$ and a subcutaneous first-order delay system are added (**Figure 2**). The CGS measures the interstitial glucose concentration. In order to consider CGM, an interstitial glucose compartment is modeled as a first-order delay system with output $Y(t)$ (**Figure 2**). This way, it is possible to include the compensation of the sensor dynamic[22] later on. In total, we obtain a dynamical mathematical model with nine states. They are summarized into state vector

$$\mathbf{x}(t) = [G(t), I(t), X(t), Y(t), v_1(t), v_2(t), q_{G1}(t), q_{G2}(t), q_I(t)]^T \quad (1)$$

In **Table 1**, the corresponding states and differential equations are summarized, and the model parameters are given for the physiological and diabetic cases. The nonlinear state space differential equation

$$\frac{d\mathbf{x}(t)}{dt} = \mathbf{f}(\mathbf{x}(t), \mathbf{u}(t)) \quad (2)$$

with input vector $\mathbf{u}(t) = [u_{GV}(t), u_{IV}(t), u_{GO}(t), u_{IS}(t)]^T$, is complemented with a linear and time-invariant measurement equation,

$$\mathbf{y}(t) = \mathbf{H}\mathbf{x}(t), \quad (3)$$

that selects the measurable outputs from the states, e.g., if plasma glucose $G(t)$ or interstitial glucose $Y(t)$ can be captured.

State Observability
Observability analysis proves which of the model states in $\mathbf{x}$ can be estimated theoretically from measurement $\mathbf{y}$. For that purpose, the Gramian observability matrix $\mathbf{W}_O$ is determined, which quantifies generalized energy transfer E_O from initial state $\mathbf{x}(0)$ to the output within an infinite time horizon:
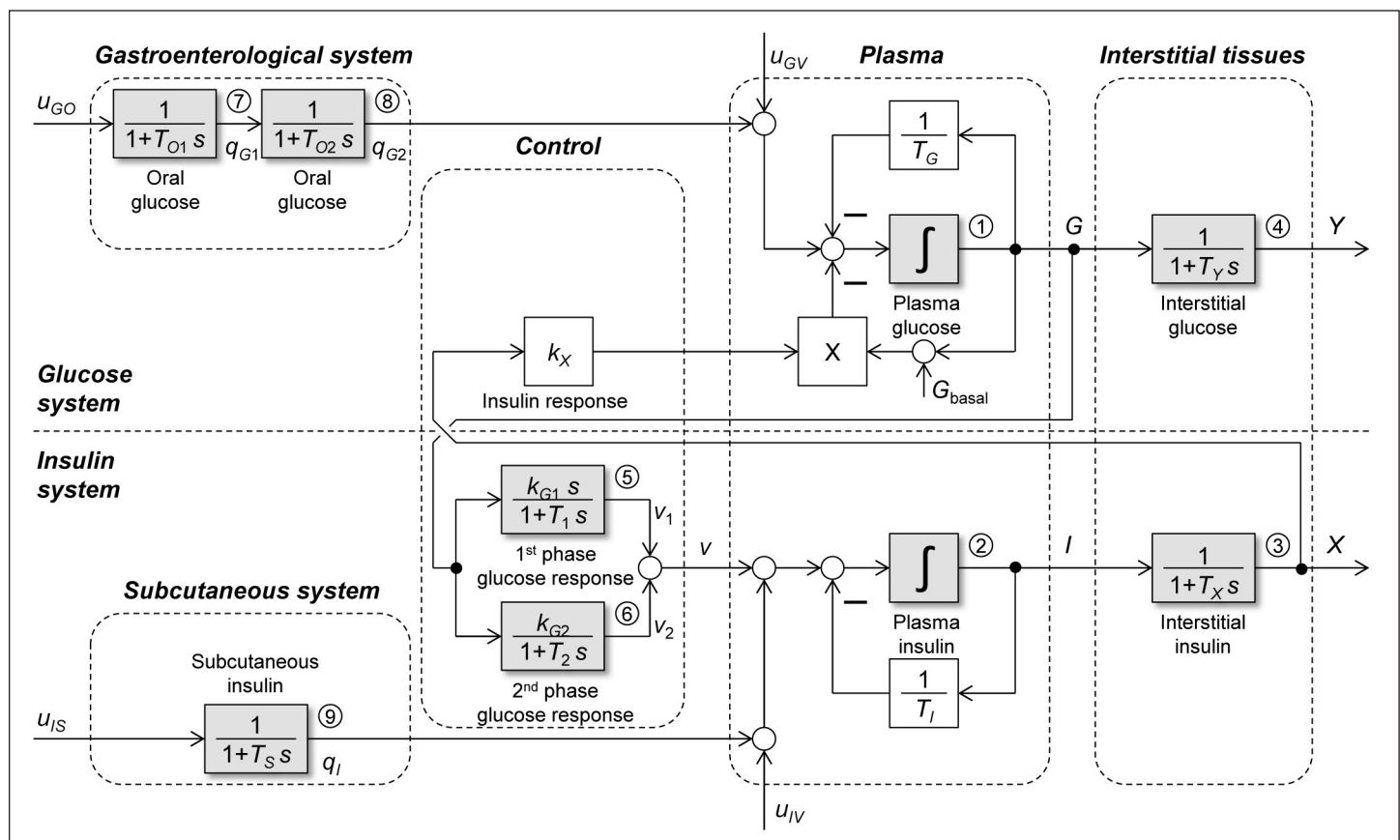

Figure 2. Block diagram of the dynamical model of the glucose–insulin homeostasis. Dynamic blocks are marked in grey.

Real-Time State Estimation and Long-Term Model Adaptation: A Two-Sided
Approach toward Personalized Diagnosis of Glucose and Insulin Levels

Eberle

Table 1.
Glucose–Insulin Model Is Defined by a Set of Nine First-Order Differential Equations[a]

Compartment	Differential equation	Maximum state x_{max}	Parameters and inputs [typical for diabetes], (source)	
1. Plasma glucose $G(t)$ in mg/dl	$\dfrac{dG(t)}{dt} = -\dfrac{1}{T_G} G(t) - k_x X(t)[G(t) + G_{basal}]$ $+ q_{G2}(t) + u_{GV}(t)$	100 mg/dl	T_G	= 32.45 [1000] min; glucose time constant (Ref. 23: $1/p_1$)
			k_X	= 507 x 10^{-6} ml/µU/mg/dl/min; insulin sensitifity (Ref. 23: p_3/p_2)
			G_{basal}	= 90 mg/dl; basal plasma glucose (Ref. 23: $G(t_{end})$)
			u_{GV}	in mg/dl/min; venous glucose input
2. Plasma insulin $I(t)$ in µU/ml	$\dfrac{dI(t)}{dt} = -\dfrac{1}{T_I} I(t) - v_1(t) + v_2(t)$ $+ q_I(t) + u_{IV}(t)$	50 µU/ml	T_I	= 3.33 min; insulin time constant (Ref. 23: $1/n$)
			u_{IV}	input in µU/ml/min; venous insulin input
			I_{basal}	= 9µU/ml; basal plasma insulin, Ref. 23.
3. Interstitial insulin $X(t)$ in µU/ml	$\dfrac{dX(t)}{dt} = -\dfrac{1}{T_X} X(t) + \dfrac{1}{T_X} I(t)$	10 µU/ml	T_X	= 47.78 min; interstitial insulin time constant (Ref. 23: $1/p_2$)
4. Interstitial glucose $Y(t)$ in mg/dl	$\dfrac{dY(t)}{dt} = -\dfrac{1}{T_Y} Y(t) + \dfrac{1}{T_Y} G(t)$	50 µU/ml	T_Y	= 16.0 min; interstial glucose time constant (modified from Reference 4; τ = 20.3 min)
5. First-phase glucose response $v_1(t)$ in µU/ml/min	$\dfrac{dv'_1(t)}{dt} = -\dfrac{1}{T_1} v'_1(t) - \dfrac{k_{G1}}{T_1^2} G(t),$ $v_1(t) = v'_1(t) + \dfrac{k_{G1}}{T_1} G(t)$	20 µU/ml/min	T_1	= 4.0 min; first-phase time constant (definition)
			k_{G1}	= 1.080 [0] dl/mg/µU/ml; first-phase glucose sensitivity (definition), remark; k_{G1} is multiplied by factor 20 in case of oral excitation to model the incretin effect[24]
6. Second-phase glucose response $v_2(t)$ in µU/ml/min	$\dfrac{dv_2(t)}{dt} = -\dfrac{1}{T_2} v_2(t) + \dfrac{k_{G2}}{T_2} G(t)$	10 µU/ml/min	T_2	= 12.0 min; second-phase time constant (definition)
			k_{G2}	= 0.107 [0] dl/mg/µU/ml/min; second-phase glucose sensitivity (definition)
7. Oral glucose flow (1) $q_{G1}(t)$ in mg/dl/min	$\dfrac{dq_{G1}(t)}{dt} = -\dfrac{1}{T_{O1}} q_{G1}(t) + \dfrac{1}{T_{O1}} u_{GO}(t)$	10 mg/dl/min	T_{O1}	= 15.0 min; first oral time constant (definition)
			u_{GO}	input in mg/dl/min; oral glucose input
8. Oral glucose flow (2) $q_{G2}(t)$ in mg/dl/min	$\dfrac{dq_{G2}(t)}{dt} = -\dfrac{1}{T_{O2}} q_{G2}(t) + \dfrac{1}{T_{O2}} q_{G1}(t)$	10 mg/dl/min	T_{O2}	= 60.0 min; second oral time constant (definition)
9. Subcutaneous insulin flow $q_I(t)$ in µU/ml/min	$\dfrac{dq_I(t)}{dt} = -\dfrac{1}{T_S} q_I(t) + \dfrac{1}{T_S} u_{IS}(t)$	30 µU/ml/min	T_S	= 20.0 min; subcutaneous insulin time constant (definition)
			u_{IS}	input in µU/ml/min; subcutaneous insulin input

[a] Only the first-order differential equation is nonlinear.

$$E_O = \int_0^\infty \mathbf{y}^T(\tau)\mathbf{y}(\tau)d\tau = \mathbf{x}^T(0)\mathbf{W}_O\mathbf{x}(0) \quad (4)$$

For the case of a nonlinear system as defined in **Equation (2)**, $\mathbf{W}_O$ can be approximated by the *empirical observability Gramian*.[25] We have previously summarized its calculation.[21] For nonlinear systems, observability not only is a system property, but it also depends on the specific state trajectory. For the subsequent analysis, we normalize each state such that its energy transfer to the output is equal to one.

Next, a singular value decomposition of empirical observability Gramian $\lambda(\mathbf{W}_O)$ allows assessing observability. The largest singular value $\overline{\lambda}$ rates the energy transfer from a single state with the best possible observability. On the other hand, the smallest singular value $\underline{\lambda}$ quantifies the energy transfer from the least observable state to the outputs. It characterizes the "bottleneck" of observability and will be considered in the following. A system is unobservable, if $\underline{\lambda}$ is zero. We assume that a system is practically observable if the energy transfer from the least observable state does not

Real-Time State Estimation and Long-Term Model Adaptation: A Two-Sided
Approach toward Personalized Diagnosis of Glucose and Insulin Levels

Eberle

drop below 10%. If λ is less than 0.1 for the normalized system, the signal-to-noise ratio might be too small for a reliable state estimation.

In a complex system, not all states may be observable from measurement, but this is not necessary. Only those states in $\mathbf{x}$ that are uncertain due to distortion or due to unknown initial conditions and those states that are corrected by the measurement have to be estimated. These states are summarized in $\mathbf{x}_E$. To analyze the observability corresponding to the state subset in $\mathbf{x}_E$, the rows and columns in $\mathbf{W}_O$ corresponding to those states not included in $\mathbf{x}_E$ are removed. This way, the observability of different state selections $\mathbf{x}_E$ can be analyzed until the best subset is found.

Real-Time State Estimation

An estimation algorithm allows solving the inverse problem of estimating unknown internal states from measurement by deploying the model. The central unscented Kalman filter (UKF) algorithm is appropriate in the case of nonlinear state equations.[26] For each time-discrete iteration, a prediction and a correction step has to be processed.[27] With respect to the implementation under real-time conditions, e.g., on a small micro-controller platform, the following points should be considered:

1. The prediction step has been applied only to dynamics states, summarized as x_D. States derived from parameters or inputs are usually considered to be constant in time (see the next subsection) and can be omitted.

2. Complementarily, the correction step has only been applied to states x_E to be estimated.

3. Output **Equation (3)** is linear. Therefore, a linear Kalman filter is sufficient in the correction step.

4. If there is only a scalar measurement from one sensor, e.g., $Y(t)$, no matrix inversion is necessary in the correction step.

In order to assess estimation quality, the output residual between output $\mathbf{y}(k)$ and its estimator prediction $\hat{\mathbf{y}}(k)$ can be considered:

$$\mathbf{res}(k) = \mathbf{y}(k) - \hat{\mathbf{y}}(k) \tag{5}$$

Extension to the Estimation of Parameters and Inputs

It may occur that not only model states are unknown, but model parameters or model inputs may also be unknown, such that their estimation would be of interest. For that purpose, the estimation approach can be extended by modification of the estimator model.

In order to change model parameter p into corresponding state $x_p(t)$, first, the state vector is extended and, second, in $\mathbf{f}$, parameter p is replaced by $x_p(t)$:

$$\frac{d}{dt}\begin{bmatrix} \mathbf{x}(t) \\ x_p(t) \end{bmatrix} = \begin{bmatrix} \mathbf{f}(\mathbf{x}(t),\, \mathbf{u}(t))|_{x_p(t)\,=\,p} \\ 0 \end{bmatrix} \tag{6}$$

In order to change unknown input $u_i(t)$ into a state, first, $u_i(t)$ is separated from remaining input $\mathbf{u}_{red}(t)$,

$$\mathbf{u}(t) = \begin{bmatrix} \mathbf{u}_{\text{red}}(t) \\ u_i(t) \end{bmatrix} \tag{7}$$

second, new state $x_u(t)$ is added to state vector $\mathbf{x}(t)$; and, third, in $\mathbf{f}$, former input $u_i(t)$ is replaced by new state $x_u(t)$,

$$\frac{d}{dt}\begin{bmatrix} \mathbf{x}(t) \\ x_u(t) \end{bmatrix} = \begin{bmatrix} \mathbf{f}(\mathbf{x}(t),\, \mathbf{u}_{\text{red}}(t))|_{x_u(t)\,=\,u_i(t)} \\ 0 \end{bmatrix} \tag{8}$$

Note that, by these changes, new nonlinearities will be introduced into the extended system. Nevertheless, the extended system can be deployed for estimation (see Real-Time State Estimation) if observability is ensured sufficiently (see State Observability).

Results

Prediction

For the purpose of model validation, **Figure 3** shows four typical simulated scenarios. An IVGTT is simulated for a nondiabetic subject as scenario 1. A first and second insulin response is observed in $I(t)$, and a fast degradation of the plasma glucose peak is shown in $G(t)$. Subcutaneous glucose $Y(t)$ follows with a certain delay. Scenario 2 simulates the reaction of an oral glucose administration to a nondiabetic subject as an OGTT. Compared with scenario 1, a delayed response is observed as a consequence of two mechanisms; model compartments 7 and 8 (see **Figure 2**) describe a delayed oral glucose ingestion. Additionally, an increased first-phase glucose sensitivity (see **Table 1**) is damping
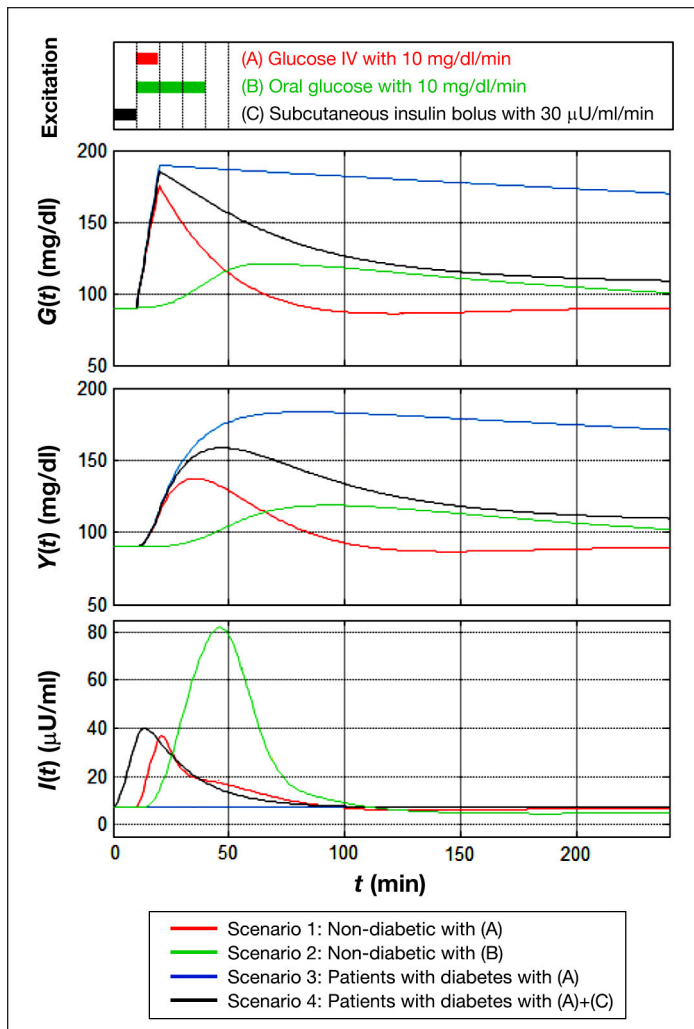
Real-Time State Estimation and Long-Term Model Adaptation: A Two-Sided
Approach toward Personalized Diagnosis of Glucose and Insulin Levels

Eberle

Figure 3. Simulation of the model defined in **Figure 2**, with parameters shown in **Table 1** and sampling time $\Delta t = 1$ min. Plasma glucose $G(t)$, subcutaneous glucose $Y(t)$, and plasma insulin $I(t)$ are shown. Scenarios: (1) IVGTT (red line) and (2) OGTT of a nondiabetic subject (green line), (3) IVGTT of a subject with diabetes (blue line), which is added in (4) with an insulin bolus (black line).

Figure 4. Simulation scenarios (dashed curves) are compared with measured data (solid curves) from pigs.[11] The model is defined in **Figure 2**, with parameters shown in **Table 1** and sampling time $\Delta t = 2.5$ min. It is assumed $G_{basal} = 60$ mg/dl. Scenarios: (5) Nondiabetic subject with data from Figure 2a of Reference 11 (red line), (6) subject with diabetes without insulin bolus with data from Figure 2c of Reference 11 (green line), and (7) subject with diabetes with insulin bolus with data Figure 3a of Reference 11 (black line).

plasma glucose levels in the case of oral excitation, which is necessary to incorporate the incretin effect.[27] A justification for this model parameter adaption will be given in Parameter Identification and Model Adaptation. In contrast, the diabetic system of scenario 3 is not able to reduce glucose after IVGTT sufficiently. Finally, an insulin bolus after 30 min is simulated in scenario 4. As a consequence, glucose decreases in the subject with diabetes.

In **Figure 4**, simulated scenarios are compared with measured data from pigs.[11] Starting with a basal plasma glucose of $G_{basal} = 60$ mg/dl, the system is triggered by oral glucose within the first 40 min. Scenarios 5 and 6 show that the model characterizes the nondiabetic and
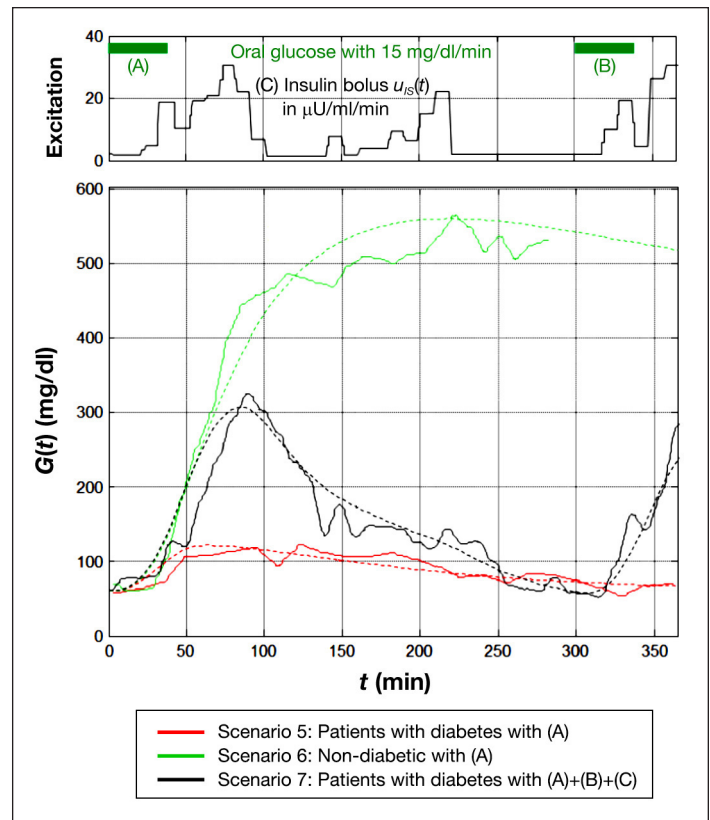
diabetic cases in good agreement, respectively. In scenario 7, an insulin bolus and a further oral glucose dosage after 300 min is applied. The model is able to simulate the impact of the insulin bolus, and the simulated plasma glucose keeps below that of scenario 6. Although the model parameters are not adjusted to the individual yet, characteristic reactions can be reproduced.

Observability

The observability of the system's states should be analyzed according to State Observability for the four scenarios introduced in **Figure 3**. Resulting smallest singular values $\underline{\lambda}(\mathbf{W}_O)$ of different state subsets $\mathbf{x}_E$ are shown in **Figure 5** as a bar diagram. The observability based on the measurement of $Y(t)$, e.g., by a CGS, is compared with the direct measurement of only plasma glucose $G(t)$.

If $Y(t)$ is measured, one of signals $G(t)$, $I(t)$, or $X(t)$ can be estimated beside $Y(t)$ itself, as shown in cases a, b, and c

Real-Time State Estimation and Long-Term Model Adaptation: A Two-Sided
Approach toward Personalized Diagnosis of Glucose and Insulin Levels

Eberle

in **Figure 5**. If plasma glucose and insulin should be estimated (cases d and e), this is only possible in the nondiabetic system. The estimation of further states (cases f and g) mostly violates practical observability. The last case (h) illustrates that observability will break down if two closely dependent states should be estimated, as this is the case for $I(t)$ and $X(t)$. These signals could not be separated based on the measurement of $Y(t)$. Hence only one of them should be estimated as in cases a and c.

The situation can be improved if $G(t)$ is measured directly instead of $Y(t)$ in cases d, e, and f, which is shown in **Figure 5** as empty bars.

Real-Time Estimation

Kalman filter estimation is mostly applied to the glucose subsystem only.[5,28–30] In order to analyze the signal estimation in the whole glucose–insulin system, we recall scenarios 5 and 6. An UKF (see Real-Time State Estimation) is designed for estimation of state subset $x_E(t) = [G(t) \ I(t)]^T$, case d. The details are given in **Table 2** and Reference 25.

As could be expected, the estimator filters the measured glucose signal soundly (**Figure 6**). But this is not the main achievement of the estimation. Moreover, it provides the full state vector throughout the time. As an example, at the time point $t_0 = 60$ min, a model-based prediction is

started, which might be used to assess therapies. If the full state information is used to start the prediction in t_0, the result is much better than using only the initial value for plasma glucose (**Figure 6**).

Parameter Identifiability

For the long-term identification and adaptation of model parameters, their identifiability has to be ensured. For assessment, all 13 model parameters (**Table 1**) are converted into states without dynamics following **Equation (6)**. We obtain new state vector $[x \ x_P]^T$ of dimension 22. Of course, not all entries can be identified from a single measurement, and we have to determine the degree of observability of state subsets x_E using the methods already applied in Observability. **Figure 7** displays the smallest singular value as measures of observability for different subsets x_E.

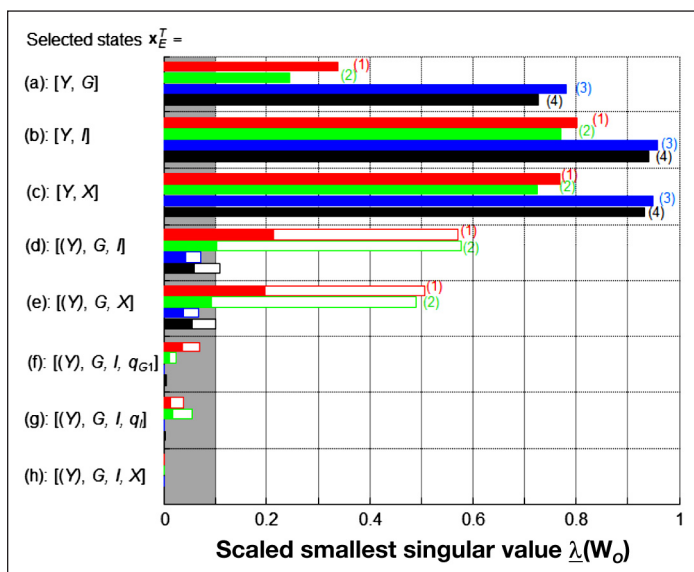| Table 2. Setup of the Unscented Kalman Filter	
Initial states	$\hat{x}(0) = O^T$
Maximum states	x_{max}; see **Table 1**
Initial covariance matrix	$\hat{P}(0) = \text{diag}(x^2_{max})$
State noise covariance matrix	$Q = \text{diag}((0.01x_{max})^2)$ for measured state multiplied by factor 100
Measurement noise covariance matrix	R diagonal matrix with $r_{i,i} = (3 \text{ mg/dl})^2$

Figure 5. Scaled smallest singular values of the empirical Gramian observability matrix corresponding to state subset x_E based on the measurement of only $Y(t)$ (filled bars) or of only $G(t)$ (empty bars) for scenarios 1 to 4. A subset achieving less than 0.1 is considered to no longer observable.
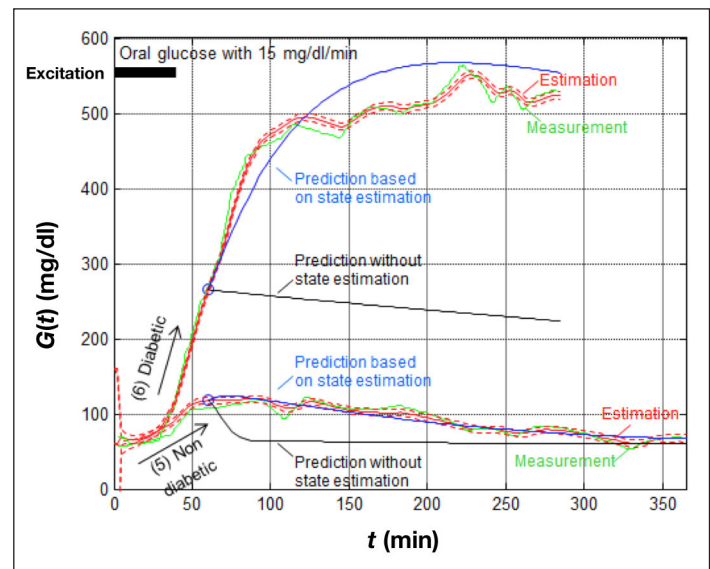

Figure 6. The measurements of Figure 2a of Reference 11 (scenario 5) and Figure 2c of Reference 11 (scenario 6) are used for state estimation. The estimation (with its standard deviation as dashed curve) filters the measurement with sampling time $\Delta t = 2.5$ min. At time $t_0 = 60$ min, a model-based prediction is started with and without the full state information.

Real-Time State Estimation and Long-Term Model Adaptation: A Two-Sided
Approach toward Personalized Diagnosis of Glucose and Insulin Levels

Eberle

Starting from case d (also shown in **Figure 5**), different parameters are added for estimation in cases i to o of **Figure 7**. For internal model parameters T_I, T_X, T_G, k_{G1}, and k_{G2}, it can be seen that identifiability highly depends on the underlying scenario. Where identifiability is ensured in the most nondiabetic scenarios (1 and 2), it fails for the diabetic scenarios (3 and 4). For scenarios 1 and 2, identifiability can be improved if $G(t)$ is measured instead of $Y(t)$.

The identifiability of peripheral model parameters depends on the local measurement or excitation. Parameter T_Y is only identifiable if $Y(t)$ is measured (filled bars in case m), and T_S can only be identified in scenario 4 with a subcutaneous insulin excitation (see case n). In the same way, parameter T_{O2} depends on an oral glucose excitation and is only identifiable for scenario 2 (see case o).

In **Figure 7**, these cases are repeated, but the estimation of $I(t)$ is removed, which is denoted as cases i*–o*. Identifiability is improved in all cases. Especially diabetic scenarios gain identifiability; compare, for example, cases j and j*.
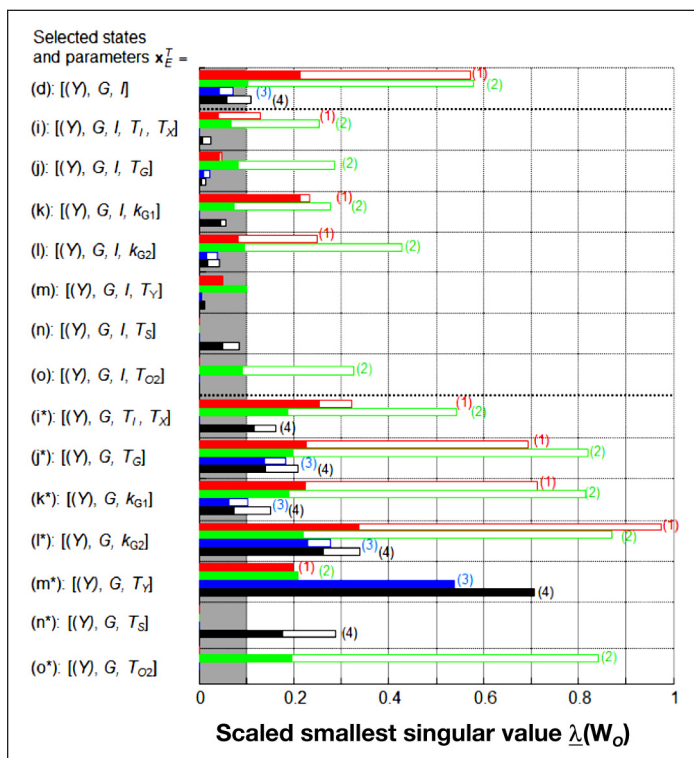
Parameter Identification and Model Adaptation

To demonstrate parameter identification, we pick up scenarios 5 to 7 based on previous data.[11] In **Figure 8a**, the estimation of first-phase glucose sensitivity k_{G1} according to case k* in **Figure 7** is shown. Starting with the default value of k_{G1} from **Table 1**, its value is increasing by approximate factor 20. This might be interpreted as incretin effect, which is observed in the case of oral glucose administration.[24]

Figures 8b to **8d** show the estimation of second-phase glucose sensitivity k_{G2} according to case l* in **Figure 7**. As expected, the initial value of k_{G2} is only slightly adjusted for nondiabetic scenario 5. But in diabetic cases 6 and 7, gain k_{G2} is adjusted within approximately 2 h to almost zero, which characterizes the diabetic situation correctly.

It shows that an individualized parameter adaption and a long-term adaptation of the initial model are possible. This will allow personalizing an initial standard
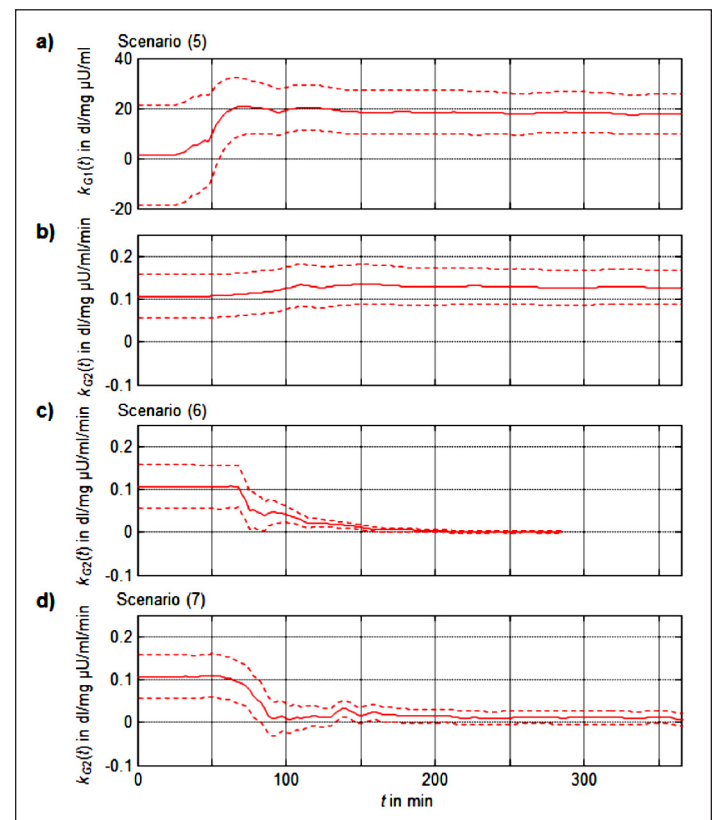
Figure 7. Scaled smallest singular values of the empirical Gramian observability matrix corresponding to state and parameter subset $\mathbf{x}_E$ based on the measurement of $Y(t)$ (filled bars) or of only $G(t)$ (empty bars) for scenarios 1–4. A subset achieving less than 0.1 is considered to be no longer observable.

Figure 8. Parameter estimation of k_{G2} in scenario 6 with data from Figure 2c of Reference 11 (**a**) with sampling time $\Delta t = 2.5$ min, estimation result starting initially with $k_{G2,0} = 0.107$ dl/mg/μU/ml/min and ending with $k_{G2,1} = 0.0025$ dl/mg/μU/ml/min (with its standard deviation as dashed curve). (**b**) Assessment of estimation by the difference of estimation residuals res_1 with $k_{G2,1}$ and res_0 with $k_{G2,0}$ according to **Equation (5)**.

Real-Time State Estimation and Long-Term Model Adaptation: A Two-Sided
Approach toward Personalized Diagnosis of Glucose and Insulin Levels

Eberle

model to a patient-specific profile. The development of parameters k_{G1} and k_{G2} may also support diagnosis.

Observability of Inputs

Following **Equations (7)** and **(8)**, model inputs may also be estimated if they are not given as known external signals. This might be of specific interest in order to estimate external glucose input [either intravenous using $u_{GV}(t)$ or oral via $u_{GO}(t)$; see **Figure 2**]. In the same way, it might be possible to estimate an insulin bolus for diabetes patients [either intravenous using $u_{IV}(t)$ or subcutaneous via $u_{IS}(t)$; see **Figure 2**]. The results of the observability analysis of the extended systems are displayed in **Figure 9** for scenarios 1 to 4. Starting from case d, which is also shown in **Figure 5**, each of the four possible inputs is added to set $\mathbf{x}_E$ as cases p to s. As in case d, practical observability is only given for nondiabetic scenarios 1 and 2, but not for diabetic cases 3 and 4. If the estimation of plasma insulin $I(t)$ is skipped, practical observability is achieved for all inputs and scenarios; see cases p* to s* in **Figure 9**.

Estimation of Inputs

We recall simulated scenarios 1–4. Using the simulated output of interstitial glucose concentration $Y(t)$ as measurement, we now try to reconstruct the corresponding inputs by estimation. For scenarios 1 and 3, it can be
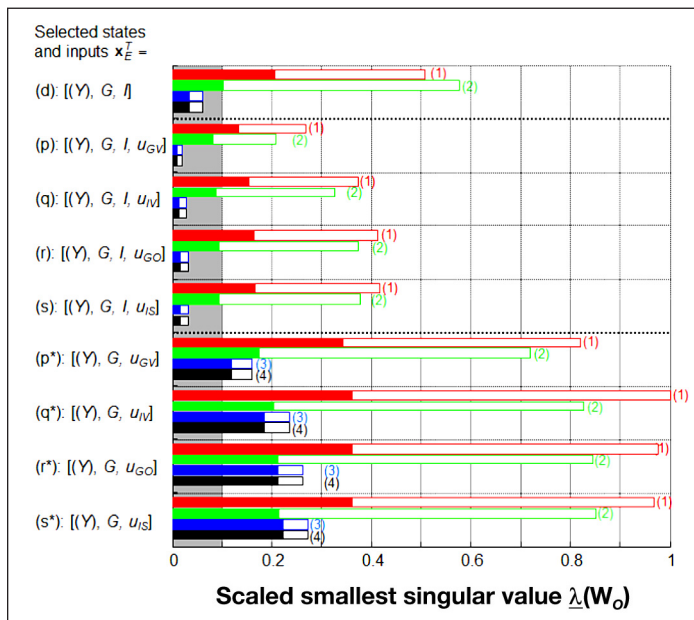
seen in **Figure 10** that the estimation of an intravenous glucose application can be estimated successfully. Obviously, this is possible for nondiabetic as well as diabetic scenarios.

In contrast, the results for scenario 2 are not satisfactory. The oral glucose dosage is estimated with a delay of approximately 60 min. Here the modeled time delay from oral to plasma glucose hinders a timely estimation of the oral glucose input, even if this input is practically observable. For completeness, **Figure 10** also shows the estimation of a subcutaneous insulin input within scenario 4. The results are unstable, and the estimated
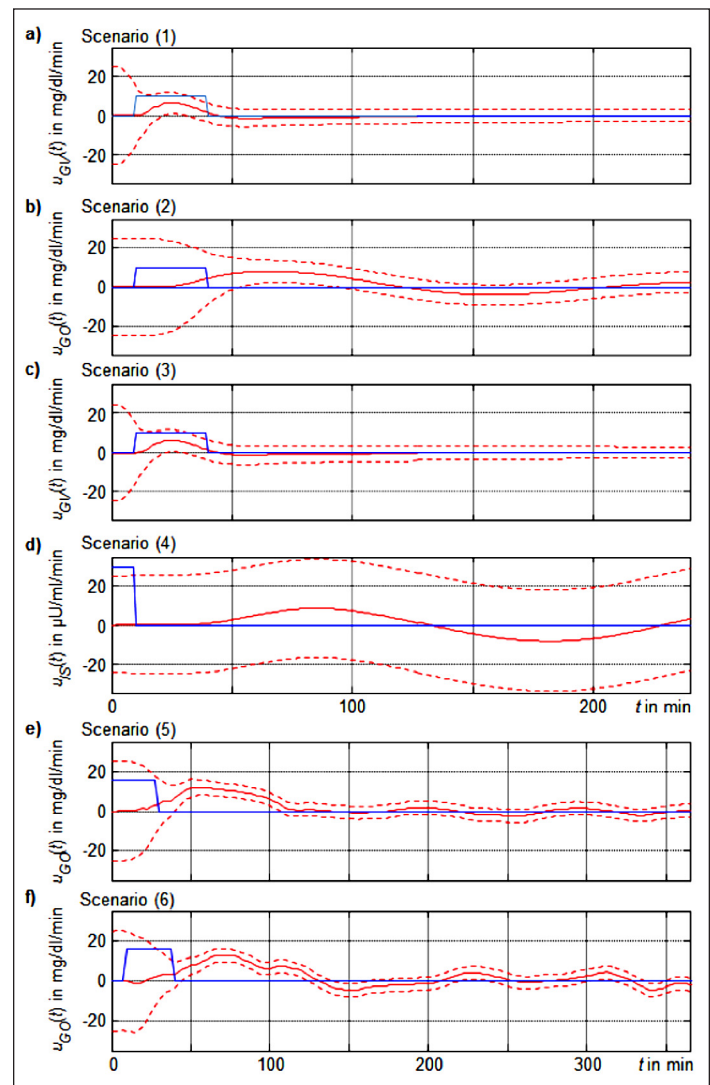

Figure 9. Scaled smallest singular values of the empirical Gramian observability matrix corresponding to state and input subset x_E based on the measurement of $Y(t)$ (filled bars) or of only $G(t)$ (empty bars) for scenarios 1–4. A subset achieving less than 0.1 is considered to be no longer observable.

Figure 10. (**a**)–(**d**) Estimation of inputs for simulated scenarios 1 to 4 (mean estimate as solid curve, standard deviation from mean as dashed curve) with sampling time $\Delta t = 1$ min. (**e**)–(**f**) Estimation of oral glucose input for scenarios 5 and 6 with sampling time $\Delta t = 2.5$ min. Data obtained from Figures residual 2a and 2c, respectively, of Reference 11 (mean estimate as solid curve, standard deviation from mean as dashed curve).

Real-Time State Estimation and Long-Term Model Adaptation: A Two-Sided
Approach toward Personalized Diagnosis of Glucose and Insulin Levels

Eberle

standard deviation does not converge. But in real application, the estimation of insulin will not be of major interest, because it is usually known as control signal within a diabetes therapy.

These results are supported by the estimations based on the measurement of real plasma glucose $G(t)$ data,[11] shown in **Figure 10** as scenarios 5 and 6. In both scenarios, a glucose input peak is observed correctly that yields from the glucose dosage, but it is delayed again for approximately 60 min.

This shows the limits of the model-based diagnoses based on the measurement of interstitial glucose $Y(t)$ or plasma glucose $G(t)$. From these signals, the oral glucose input cannot be estimated in time. It will be necessary to provide this additionally as external information for insulin control.[31]

Discussion

Using a mathematical dynamical model of the glucose–insulin homeostasis, it is possible to estimate internal model states such as plasma insulin $I(t)$. This can be provided for diagnostic purposes. A complete estimate of the system's state is especially required in real time for a precise prediction of the signal. Model-predictive control (MPC) can be applied to find an optimal insulin bolus[12,24,32,33] for diabetes patients. The MPC algorithm is based on these predictions. Hence the precise estimate of the metabolic state is an essential step toward closed-loop insulin control of diabetes patients.

In parallel, it is possible to identify selected subsets of the 13 model parameters. This way, the model can be adapted to individual patients. Starting with standard models, which may already consider metabolic disorders, e.g., diabetes type 2, the model can be adapted to the patient within a number of days. The adapted model then ensures improved signal estimation. Moreover, the development of model parameters can be used for diagnosis, e.g., a beta-cell distortion will result in decreasing loop gains k_{G1} and k_{G2}.

Precondition for state observation and parameter identification is a time-continuous measurement. With a CGS, this is now available for interstitial glucose $Y(t)$. Comparing observability between plasma glucose $G(t)$ and interstitial glucose $Y(t)$ measurement (empty versus filled bars in **Figures 5**, **7**, and **9**), it becomes obvious that the information from $Y(t)$ is limited. Beside the estimation of $G(t)$, only one further state or parameter

can be estimated, which might be $I(t)$, T_G, k_{G1}, k_{G2}, and T_Y in cases d, j*, k*, l*, and m* of **Figure 7**, respectively.

It turns out that the estimation of external inputs as an oral glucose dosage is limited. It is estimated correctly, but with a time delay,[34] such that a real-time compensation will not be possible. This has to be provided to an insulin controller separately.

Conclusions

The authors propose that the twofold strategy of real-time signal estimation combined with a long-term patient-specific parameter identification obtains the most profit from a CGS.[1] It allows a personalized diagnosis of the glucose–insulin system. As such, it will be an important module within a personalized closed-loop insulin control.

Complementary to the theoretical results presented in this contribution, a broader data analysis of a group of patients with and without diabetes will be necessary in order to find out about the distribution of model parameters. Based on this, the most important parameters have to be selected, and automated identification algorithms can be developed.

References:

1. Russell SJ. Continuous glucose monitoring awaits its "killer app". J Diabetes Sci Technol. 2008;2(3):490–4.

2. Kovatchev BP, King C, Breton M, Anderson S, Clarke W. Clinical assessment and mathematical modeling of the accuracy of continuous glucose sensors (CGS). Conf Proc IEEE Eng Med Biol Soc. 2006;1:71–4.

3. Kovatchev B, Clarke W. Peculiarities of the continuous glucose monitoring data stream and their impact on developing closed-loop control technology. J Diabetes Sci Technol. 2008;2(1):158–63.

4. Facchinetti A, Sparacino G, Cobelli C. Reconstruction of glucose in plasma from interstitial fluid continuous glucose monitoring data: role of sensor calibration. J Diabetes Sci Technol. 2007;1(5):617–23.

5. Knobbe EJ, Buckingham B. The extended Kalman filter for continuous glucose monitoring. Diabetes Technol Ther. 2005;7(1):15–27.

6. Kuure-Kinsey M, Palerm CC, Bequette BW. A dual-rate Kalman filter for continuous glucose monitoring. Conf Proc IEEE Eng Med Biol Soc. 2006;1:63–6.

7. Palerm CC, Bequette BW. Hypoglycemia detection and prediction using continuous glucose monitoring-a study on hypoglycemic clamp data. J Diabetes Sci Technol. 2007;1(5):624–9.

Real-Time State Estimation and Long-Term Model Adaptation: A Two-Sided
Approach toward Personalized Diagnosis of Glucose and Insulin Levels

Eberle

8. Facchinetti A, Sparacino G, Cobelli C. Enhanced accuracy of continuous glucose monitoring by online extended kalman filtering. Diabetes Technol Ther. 2010;12(5):353–63.

9. Facchinetti A, Sparacino G, Cobelli C. An online self-tunable method to denoise CGM sensor data. IEEE Trans Biomed Eng. 2010;57(3):634–41.

10. Facchinetti A, Sparacino G, Cobelli C. Online denoising method to handle intraindividual variability of signal-to-noise ratio in continuous glucose monitoring. IEEE Trans Biomed Eng. 2011;58(9):2664–71.

11. El-Khatib FH, Jiang J, Damiano ER. A feasibility study of bihormonal closed-loop blood glucose control using dual subcutaneous infusion of insulin and glucagon in ambulatory diabetic swine. J Diabetes Sci Technol. 2009;3(4):789–803.

12. Chee F, Fernando T, van Heerden PV. Closed-loop glucose control in critically ill patients using continuous glucose monitoring system (cgms) in real time. IEEE Trans Inf Techn Biomed. 2003;7(1):43–53.

13. Clarke WL, Anderson S, Breton M, Patek S, Kashmer L, Kovatchev B. Closed-loop artificial pancreas using subcutaneous glucose sensing and insulin delivery and a model predictive control algorithm: the virginia experience. J Diabetes Sci Technol. 2009;3(5):1031–8.

14. El-Khatib FH, Jiang J, Damiano ER. Adaptive closed-loop control provides blood-glucose regulation using dual subcutaneous insulin and glucagon infusion in diabetic swine. J Diabetes Sci Technol. 2007;1(2):181–92.

15. Finan DA, Doyle FJ 3rd, Palerm CC, Bevier WC, Zisser HC, Jovanovic L, Seborg DE. Experimental evaluation of a recursive model identification technique for type 1 diabetes. J Diabetes Sci Technol. 2009;3(5):1192–202.

16. El-Khatib FH, Russell SJ, Nathan DM, Sutherlin RG, Damiano ER. A bihormonal closed-loop artificial pancreas for type 1 diabetes. Sci Transl Med. 2010;2(27):27ra27.

17. Leal Y, Garcia-Gabin W, Bondia J, Esteve E, Ricart W, Fernández-Real JM, Vehí J. Real-time glucose estimation algorithm for continuous glucose monitoring using autoregressive models. J Diabetes Sci Technol. 2010;4(2):391–403.

18. Bergman RN, Ider YZ, Bowden CR, Cobelli C. Quantitative estimation of insulin sensitivity. Am J Physiol. 1979;236(6):E667–77.

19. Bergman RN, Phillips LS, Cobelli C. Physiologic evaluation of factors controlling glucose tolerance in man: measurement of insulin sensitivity and beta-cell glucose sensitivity from the response to intravenous glucose. J Clin Invest. 1981;68(6):1456–67.

20. Morris HC, O'Reilly B, Streja D. A new biphasic minimal model. Conf Proc IEEE Eng Med Biol Soc. 2004;1:782–5.

21. Eberle C, Ament C. Identifiability and online estimation of diagnostic parameters with in the glucose insulin homeostasis. Biosystems. 2012;107(3):135–41.

22. Breton M, Kovatchev B. Analysis, modeling, and simulation of the accuracy of continuous glucose sensors. J Diabetes Sci Technol. 2008;2(5):853–62.

23. Pacini G, Bergman RN. MINMOD: a computer program to calculate insulin sensitivity and pancreatic responsively from the frequently sampled intravenous glucose tolerance test. Comput Methods Prog Biomed. 1986;23(2):113–22.

24. Amori RE, Lau J, Pittas AG. Efficacy and safety of incretin therapy in type 2 diabetes: systematic review and meta-analysis. JAMA. 2007;298(2):194–206.

25. Geffen D, Findeisen R, Schliemann M, Allgöwer F, Guay M. Observability based parameter identifiability for biochemical reaction networks. American Control Conference, Seattle, WA, June 11–13, 2008.

26. Eberle C, Ament C. The unscented Kalman filter estimates the plasma insulin from glucose measurement. Biosystems. 2011;103(1):67–72.

27. Simon D. Optimal state estimation: Kalman, H infinity, and non-linear approaches. Hoboken: Wiley; 2006.

28. Patek SD, Breton MD, Chen Y, Solomon C, Kovatchev B. Linear quadratic gaussian-based closed-loop control of type 1 diabetes. J Diabetes Sci Technol. 2007;1(6):834–41.

29. Bequette BW. Optimal estimation applications to continuous glucose monitoring. American Control Conference, Boston, MA, 2004.

30. Bequette BW. Continuous glucose monitoring: real-time algorithms for calibration, filtering, and alarms. J Diabetes Sci Technol. 2010;4(2):404–18.

31. Gillis R, Palerm CC, Zisser H, Jovanovic L, Seborg DE, Doyle FJ. Glucose estimation and prediction through meal responses using ambulatory subject data for advisory mode model predictive control. J Diabetes Sci Technol. 2007;1(6):825–33.

32. Elleri D, Allen JM, Nodale M, Wilinska ME, Mangat JS, Larsen AM, Acerini CL, Dunger DB, Hovorka R. Automated overnight closed-loop glucose control in young children with type 1 diabetes. Diabetes Technol Ther. 2011;13(4):419–24.

33. Russell SJ, El-Khatib FH, Nathan DM, Damiano ER. Efficacy determinants of subcutaneous microdose glucagon during closed-loop control. J Diabetes Sci Technol. 2010;4(6):1288–304.

34. Dassau E, Bequette BW, Buckingham BA, Doyle FJ 3rd. Detection of a meal using continuous glucose monitoring: implications for an artificial beta-cell. Diabetes Care. 2008;31(2):295–300.